Chapter 9. Deterministic Chaos

This chapter gives a very brief review of chaotic phenomena in deterministic maps and dynamic systems with and without dissipation, and an even shorter discussion of the possible role of chaos in fluid turbulence.

9.1. Chaos in maps

Chaotic behavior of dynamic systems[1] (sometimes called the *deterministic chaos*) has become broadly recognized[2] after the publication of a 1963 paper by E. Lorenz who was examining numerical solutions of the following system of three nonlinear, ordinary differential equations,

Lorenz system

$$\begin{aligned} \dot{q}_1 &= a_1(q_2 - q_1), \\ \dot{q}_2 &= a_2 q_1 - q_2 - q_1 q_3, \\ \dot{q}_3 &= q_1 q_2 - a_3 q_3, \end{aligned} \tag{9.1}$$

as a rudimentary model for heat transfer through a horizontal liquid layer between two solid plates. (Experiment shows that if the bottom plate is kept hotter than the top one, the liquid may exhibit turbulent convection.) He has found that within a certain range of constants $a_{1,2,3}$, the solutions of Eq. (1) follow complex, unpredictable, non-repeating trajectories in the 3D q-space. Moreover, the resulting functions $q_j(t)$ (where $j = 1, 2, 3$) are so sensitive to initial conditions $q_j(0)$ that at sufficiently large times t, solutions corresponding to slightly different initial conditions are completely different.

Very soon it was realized that such behavior is typical for even simpler mathematical objects called *maps*, so that I will start my discussion of chaos from these objects. A 1D map is essentially a rule for finding the next number q_{n+1} of a sequence, in the simplest case using only its last known value q_n, in a discrete series numbered by integer index n. The most famous example is the so-called *logistic map*:[3]

Logistic map

$$q_{n+1} = f(q_n) \equiv r q_n (1 - q_n). \tag{9.2}$$

The basic properties of this map may be understood using the (hopefully, self-explanatory) graphical presentation shown in Fig. 1.[4] One can readily see that at $r < 1$ (Fig. 1a) the sequence rapidly converges to the trivial fixed point $q^{(0)} = 0$, because each next value of q is less than the previous one. However, if r is increased above 1 (as in the example shown in Fig. 1b), fixed point $q^{(0)}$ becomes unstable. Indeed, at $q_n << 1$, map (2) yields $q_{n+1} = r q_n$, so that at $r > 1$, values q_n grow with each iteration. Instead of the unstable point $q^{(0)} = 0$, in the range $1 < r < r_1$, where $r_1 \equiv 3$, the map has a stable fixed point, $q^{(1)}$, that may be found by plugging this value into both parts of Eq. (2):

---

[1] In this context, this term is understood as "systems described by deterministic differential equations".

[2] Actually, the notion of quasi-random dynamics due to the exponential divergence of trajectories may be traced back at least to (apparently independent) works by J. Poincaré in 1892 and by J. Hadamard in 1898. Citing Poincaré, "*...it may happen that small differences in the initial conditions produce very great ones in the final phenomena*. […] *Prediction becomes impossible*."

[3] Its chaotic properties were first discussed in 1976 by R. May, though the map itself is one of simple ecological models repeatedly discussed earlier, and may be traced back at least to the 1838 work by P. Verhulst.

[4] Since the maximum value of function $f(q)$, achieved at $q = ½$, equals $r/4$, the mapping may be limited by segment $x = [0, 1]$, if parameter r is between 0 and 4. Since all interesting properties of the map, including chaos, may be found within these limits, I will focus on this range.

$$q^{(1)} = rq^{(1)}(1-q^{(1)}), \tag{9.3}$$

giving $q^{(1)} = (1 - 1/r)$ – see the left branch of the plot shown in Fig. 2.

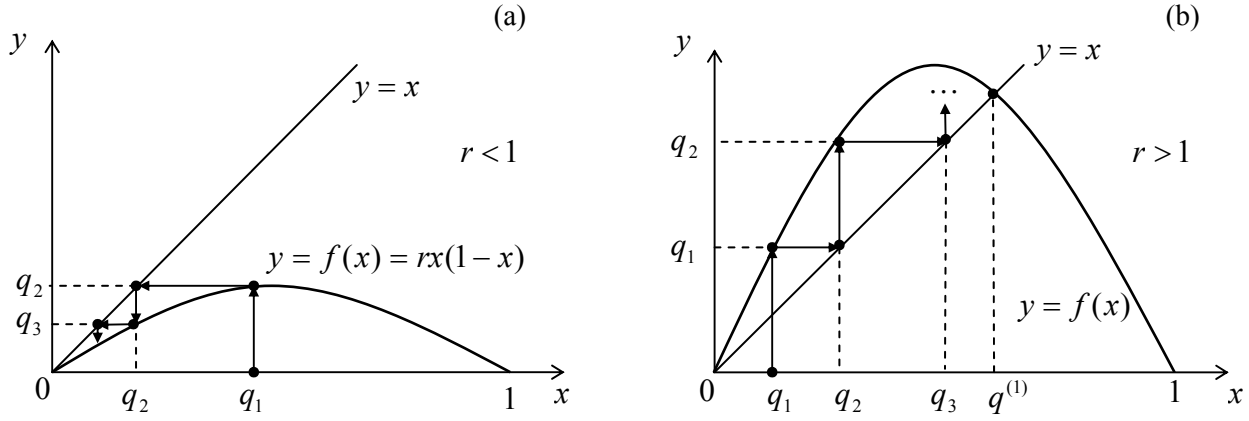

Fig. 9.1. Graphical analysis of the logistic map for: (a) $r < 1$ and (b) $r > 1$.

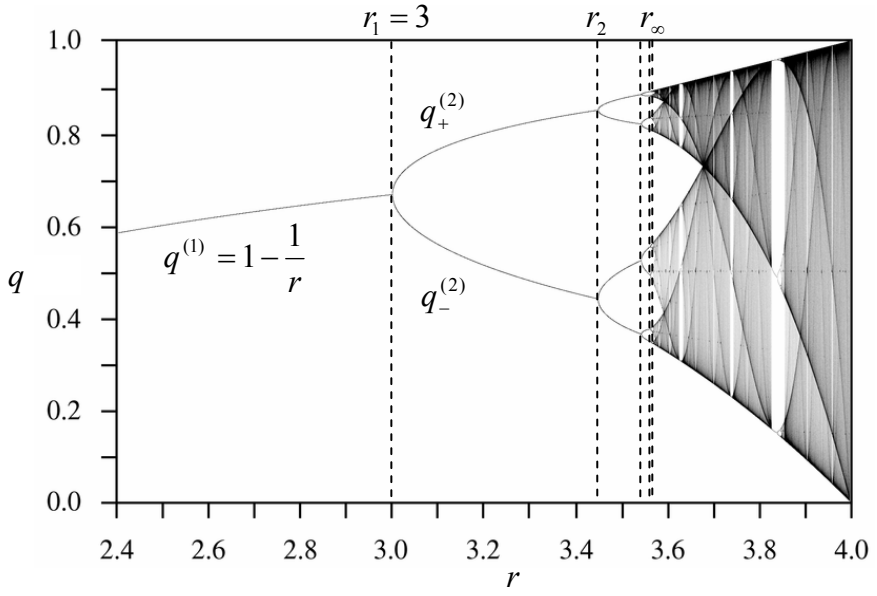

Fig. 9.2. Fixed points and chaotic regions of the logistic map. The plot is adapted from http://en.wikipedia.org/wiki/Logistic_map; a very nice live simulation of the map is also available on this Web site.

At $r > r_1 = 3$, the plot gets thicker: here the fixed point $q^{(1)}$ also becomes unstable. To prove that, let us take $q_n = q^{(1)} + \tilde{q}_n$, assume that deviation $\tilde{q}_n$ from the fixed point $q^{(1)}$ is small, and linearize map (3) in $\tilde{q}_n$, just as we repeatedly did for differential equations earlier in this course. The result is

$$\tilde{q}_{n+1} = \left.\frac{df}{dq}\right|_{q=q^{(1)}} \tilde{q}_n = r(1-2q^{(1)})\tilde{q}_n = (2-r)\tilde{q}_n. \tag{9.4}$$

It shows that $0 < 2 - r < 1$, i.e. $1 < r < 2$, deviations $\tilde{q}_n$ decrease monotonically. At $-1 < 2 - r < 0$, i.e. in the range $2 < r < 3$, the deviation signs alternate but the magnitude still decreases (as in a stable focus – see Sec. 4.6). However, at $-1 < 2 - r$, i.e. $r > r_1 = 3$, the deviations are growing by magnitude, while still changing sign, at each step. Since Eq. (2) has no other fixed points, this means that at $n \to \infty$, values

q_n do not converge to one point; rather, within the range $r_1 < r < r_2$, they approach a *limit cycle* of alternation of two points, $q_+^{(2)}$ and $q_-^{(2)}$ that satisfy the following system of algebraic equations

$$q_+^{(2)} = f(q_-^{(2)}),\ q_-^{(2)} = f(q_+^{(2)}). \tag{9.5}$$

(These points are also plotted in Fig. 2, as functions of parameter r.) What has happened at point r_1 is called the *period-doubling bifurcation*. The story repeats at $r = r_2 = 1 + \sqrt{6} \approx 3.45$ where the system goes from the 2-point limit cycle to a 4-point cycle, then at point $r = r_3 \approx 3.54$ at that the limit cycle becomes consisting of 8 alternating points, etc. Most remarkably, the period-doubling bifurcation points r_n, at that the number of points in the limit cycle doubles from 2^{n-1} points to 2^n points, become closer and closer. Numerical calculations have shown that these points obey the following asymptotic behavior:

Feigenbaum bifurcation sequence

$$r_n \to r_\infty - \frac{C}{\delta^n}, \quad \text{where } r_\infty = 3.5699..., \quad \delta = 4.6692... \tag{9.6}$$

Parameter δ is called the *Feigenbaum constant*; for other maps, and some dynamic systems (see the next section), period-doubling sequences follow a similar law, but with different parameter δ.

More important for us, however, is what happens at $r > r_\infty$. Numerous numerical experiments, repeated with increasing precision,[5] have confirmed that here the system is fully disordered, with no reproducible limit cycle, though (as Fig. 2 shows) at $r \approx r_\infty$, all sequential values q_n are still confined to a few narrow regions.[6] However, as parameter r is increased well beyond r_∞, these regions broaden and merge. This the so-called *full*, or *well-developed* chaos, with no apparent order at all.[7]

The most important feature of chaos (in this and any other system) is the *exponential divergence of trajectories*. For a 1D map, this means that even if the initial conditions q_1 in two map implementations differ by a very small amount Δq_1, the difference Δq_n between the corresponding sequences q_n is growing (on the average) exponentially with n. Such exponents may be used to characterize chaos. Indeed, let us assume that Δq_1 is so small that N first values q_n are relatively close to each other. Then an evident generalization of the first of Eqs. (4) to an arbitrary point q_n is

$$\Delta q_{n+1} = e_n \Delta q_n, \qquad e_n \equiv \left.\frac{df}{dq}\right|_{q=q_n}. \tag{9.7}$$

Using this result iteratively for N steps, we get

$$\Delta q_N = \Delta q_1 \prod_{n=1}^{N} e_n, \qquad \text{so that } \ln\left|\frac{\Delta q_N}{\Delta q_1}\right| = \sum_{n=1}^{N} \ln|e_n|. \tag{9.8}$$

[5] The reader should remember that just as the usual ("nature") experiments, numerical experiments also have limited accuracy, due to unavoidable rounding errors.

[6] The geometry of these regions are essentially *fractal*, i.e. has a dimensionality intermediate between 0 (which any final set of geometric points would have) and 1 (pertinent to a 1D continuum). An extensive discussion of fractal geometries, and their relation to the deterministic chaos may be found, e.g., in the book by B. B. Mandelbrot, *The Fractal Geometry of Nature*, W. H. Freeman, 1983.

[7] This does not mean that the chaos development is a monotonic function of r. As Fig. 2 shows, within certain intervals of this parameter chaos suddenly disappears, being replaced, typically, with a few-point limit cycle, just to resume on the other side of the interval. Sometimes (but not always!) the "route to chaos" on the borders of these intervals follows the same Feigenbaum sequence of period-doubling bifurcations.

Numerical experiments show that in most chaotic regimes, at $N \to \infty$ such a sum fluctuates about an average, which grows as λN, with parameter

$$\lambda = \lim_{\Delta q_1 \to 0} \lim_{N \to \infty} \frac{1}{N} \sum_{n=1}^{N} \ln |e_n| , \tag{9.9}$$

Lyapunov exponent

called the *Lyapunov exponent*,[8] being independent on the initial conditions. The bottom panel in Fig. 3 shows it as a function of the parameter r for the logistic map (2).

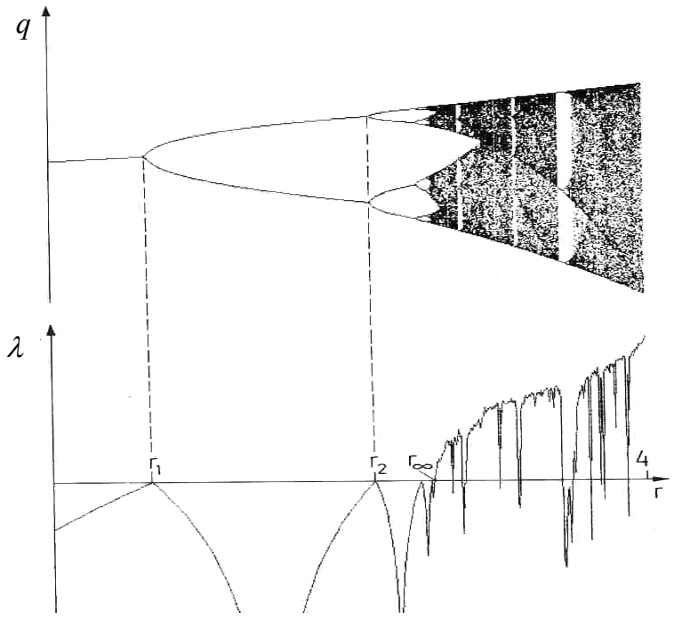

Fig. 9.3. The Lyapunov exponent for the logistic map. Adapted from the monograph by Schuster and Just (cited below). © WileyVCH Verlag GmbH & Co. KGaA.

Note that at $r < r_\infty$, λ is negative, indicating trajectory's stability, besides points r_1, r_2, … where λ would become positive if the limit cycle change had not brought it back to the negative territory. However, at $r > r_\infty$, λ becomes positive, returning the negative values only in limited intervals of stable limit cycles. It is evident that in numerical experiments (which dominate the studies of the deterministic chaos) the Lyapunov exponent may be used as a good measure of chaos' "depth".[9]

Despite all the abundance of results published for particular maps,[10] and several interesting general observations (like the existence of the Feigenbaum bifurcation sequences), to the best of my knowledge nobody can yet predict the patterns like those shown in Fig. 2 and 3, from just looking at the map rule itself, i.e. without carrying out actual numerical experiments with in. Unfortunately the situation with chaos in other systems is not much better.

[8] After A. Lyapunov (1857-1918), famous for his studies of stability of dynamic systems.

[9] N-dimensions maps, which relate N-dimensional vectors rather than scalars, may be characterized by N Lyapunov exponents rather than one. In order to have chaotic behavior, it is sufficient for just one of them to become positive. For such systems, another measure of chaos, the *Kolmogorov entropy,* may be more relevant. This measure, and its relation with the Lyapunov exponents, are discussed, e.g., in SM Sec. 2.2.

[10] See, e.g., Chapters 2-4 in H. G. Schuster and W. Just, *Deterministic Chaos*, 4th ed., Wiley-VCH, 2005, or Chapters 8-9 in J. M. T. Thompson and H. B. Stewart, *Nonlinear Dynamics and Chaos*, 2nd ed., Wiley, 2002.

9.2. Chaos in dynamic systems

Proceeding to the discussion of chaos in dynamic systems, it is more natural, with our background, to illustrate this discussion not with the Lorenz' system Eqs. (1), but with the system of equations describing a dissipative pendulum driven by a sinusoidal external force, which was repeatedly discussed in Chapter 4. Introducing two new variables, the normalized momentum $p \equiv \dot{q}/\omega_0$ and the external force's full phase $\psi \equiv \omega t$, we may rewrite Eq. (4.42) describing the pendulum,

$$\ddot{q} + 2\delta\dot{q} + \omega_0^2 \sin q = f_0 \cos\omega t\,, \tag{9.10a}$$

in a form similar to Eq. (1), i.e. as a system of three first-order ordinary differential equations:

$$\begin{aligned} \dot{q} &= \omega_0 p, \\ \dot{p} &= -\omega_0 \sin q - 2\delta p + (f_0/\omega_0)\cos\psi, \\ \dot{\psi} &= \omega. \end{aligned} \tag{9.10b}$$

Figure 4 several results of numerical solution of Eq. (10).[11] In all cases, the internal parameters δ and ω_0 of the system, and the external force amplitude f_0 are fixed, while the external frequency ω is gradually changed. For the case shown on the top panel, the system still tends to a stable periodic solution, with low contents of higher harmonics. If the external force frequency is reduced by a just few percent, the 3rd subharmonic may be excited. (This effect has already been discussed in Sec. 4.8 – see, e.g., Fig. 4.15.) The next panel shows that just a very small further reduction of frequency leads to a new tripling of the period, i.e. the generation of a complex waveform with the 9th subharmonic. Finally, even a minor further change of parameters leads to oscillations without any visible period, e.g., chaos.

In order to trace this transition, direct observation of the oscillation waveforms $q(t)$ is not very convenient, and trajectories on the phase plane $[q, p]$ also become messy if plotted for many periods of the external frequency. In situations like this, the Poincaré (or "stroboscopic") plane, already discussed in Sec. 4.6, is much more useful. As a reminder, this is essentially just the phase plane $[q, p]$, but with the points highlighted only once a period, e.g., at $\psi = 2\pi n$, with $n = 1, 2, \ldots$ On this plane, periodic oscillations of frequency ω are presented just as one fixed point – see, e.g. the top panel in the right column of Fig. 4. The beginning of the 3rd subharmonic generation, shown on the next panel, means tripling of the oscillation period, and is reflected on the Poincaré plane by splitting the fixed point into three. It is evident that this transition is similar to the period-doubling bifurcation in the logistic map, besides the fact (already discussed in Sec. 4.8) that in systems with an asymmetric nonlinearity, such as the pendulum (10), the 3rd subharmonic is easier to excite. From this point, the 9th harmonic generation (shown on the 3rd panel of Fig. 4), i.e. one more splitting of the points on the Poincaré plane, may be understood as one more step on the Feigenbaum-like route to chaos – see the bottom panel of that figure.

So, the transition to chaos in dynamic systems may be at least qualitatively similar to than in 1D maps, with the similar law (6) for the critical values of some parameter r of the system (in Fig. 4, frequency ω), though generally with a different value of exponent δ. Moreover, it is evident that we can always consider the first two differential equations of system (10b) as a 2D map that relates the vector $\{q_{n+1}, p_{n+1}\}$ of the coordinate and velocity, measured at $\psi = 2\pi(n + 1)$, with the previous value $\{q_n, p_n\}$

[11] In the actual simulation, a small term εq, with $\varepsilon << 1$, has been added to the left-hand part of this equation. This term slightly somewhat tames the trend of the solution to spread along q axis, and makes the presentation of results easier, without affecting the system dynamics too much.

of that vector (reached at $\psi = 2\pi m$). Unfortunately this similarity also implies that chaos in dynamical systems is at least as complex, and it as little understood, as in maps.

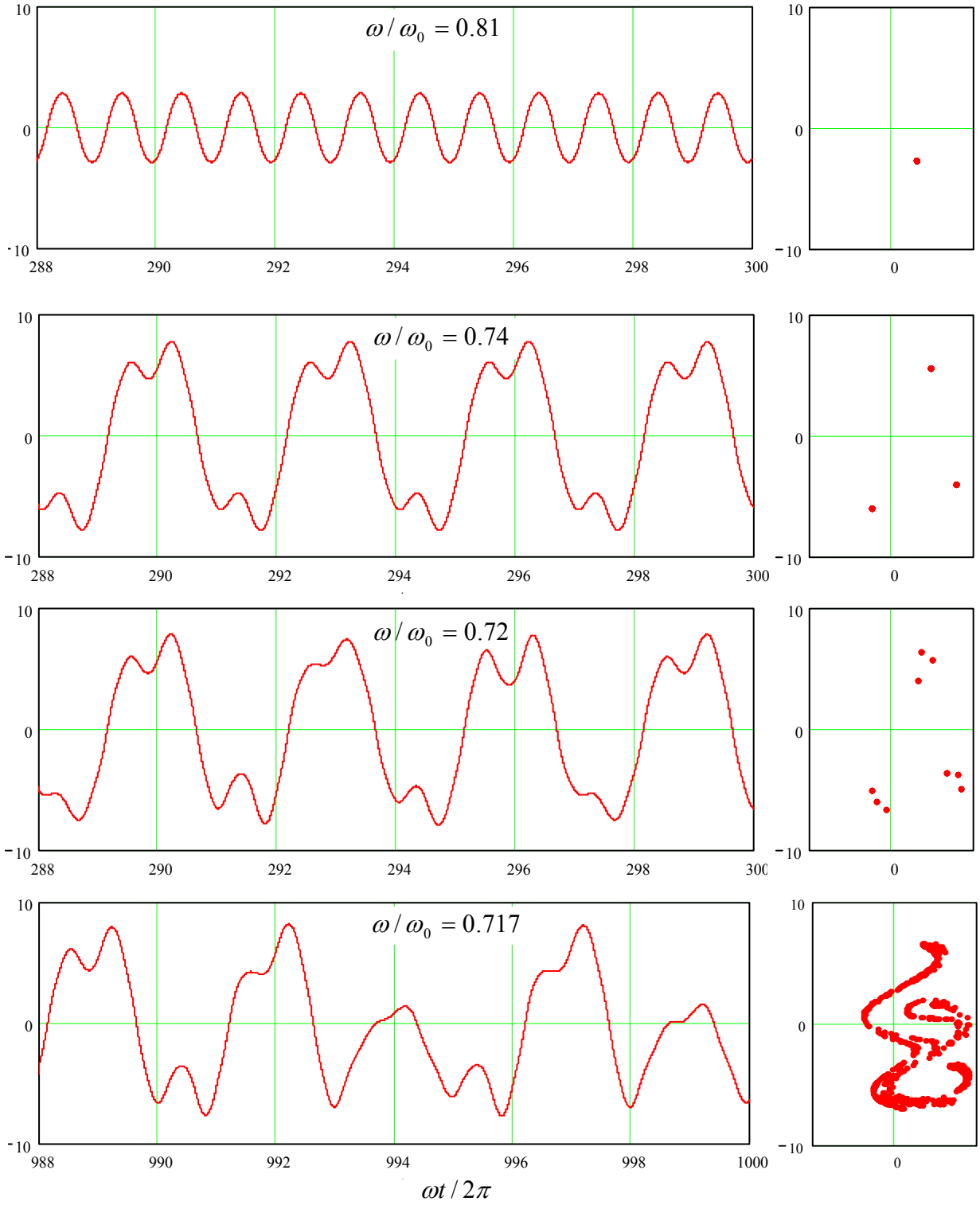

Fig. 9.4. Oscillations in a pendulum with weak damping, $\delta/\omega_0 = 0.1$, driven by a sinusoidal external force with a fixed effective amplitude $f_0/\omega_0^2 = 1$, and several close values of the frequency (listed on the panels). Left column: oscillation waveforms $q(t)$ recorded after certain initial transient intervals. Right column: representations of the same processes on the Poincaré plane of variables $[p, q]$.

For example, Fig. 5 shows (a part of) the state diagram of the externally-driven pendulum, with the red bar marking the route to chaos traced in Fig. 4, and shading/hatching styles marking different regimes. One can that the pattern is at least as complex as that shown in Figs. 2 and 3, and besides a few features,[12] is equally unpredictable from the form of the equation.

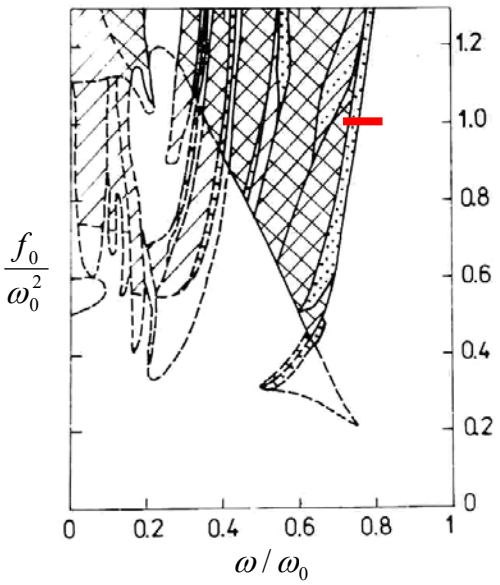

Fig. 9.5. Phase diagram of an externally-driven pendulum with $\delta/\omega_0 = 0.1$. Regions of oscillations with the basic period are not shaded. The notation for other regions is as follows. Doted: subharmonic generation; cross-hatched: chaos; hatched: chaos or basic period (depending on the initial conditions); hatch-dotted: basic period or subharmonics. Solid lines show boundaries of single-regime regions, while dashed lines are boundaries of regions in which several types of motion are possible, depending on history. (Figure courtesy V. Kornev.)

Are there any valuable general results concerning chaos in dynamic systems? The most important (though an almost evident) result is that this phenomenon is impossible in any system described by one or two first-order differential equations with right-hand parts independent of time. Indeed, let us start with a single equation

$$\dot{q} = f(q), \tag{9.11}$$

where $f(q)$ is any single-valued function. This equation may be directly integrated to give

$$t = \int^{q} \frac{dq'}{f(q')} + \text{const}, \tag{9.12}$$

showing that the relation between q and t is unique and hence does not leave place for chaos.

Now, let us explore the system of two such equations:

$$\begin{aligned} \dot{q}_1 &= f_1(q_1, q_2), \\ \dot{q}_2 &= f_2(q_1, q_2). \end{aligned} \tag{9.13}$$

Consider its phase plane shown schematically in Fig. 6. In a "usual" system, the trajectories approach either some fixed point (Fig. 6a) describing static equilibrium, or a limit cycle (Fig. 6b) describing periodic oscillations. (Both notions are united by the term *attractor*, because they "attract" trajectories launched from various initial conditions.) However, phase plane trajectories of a chaotic system of

[12] In some cases, it is possible to predict a parameter region where chaos *cannot* happen, due to lack of any instability-amplification mechanism. Unfortunately, typically the analytically predicted boundaries of such region form a rather loose envelope of the actual (numerically simulated) chaotic regions.

equations that describe real physical variables (which cannot tend to infinity), should be confined to a limited phase plane area, and simultaneously cannot start repeating each other. (This topology is frequently called the *strange attractor*.) For that, 2D trajectories need to cross – see, e.g., point *A* in Fig. 6c.

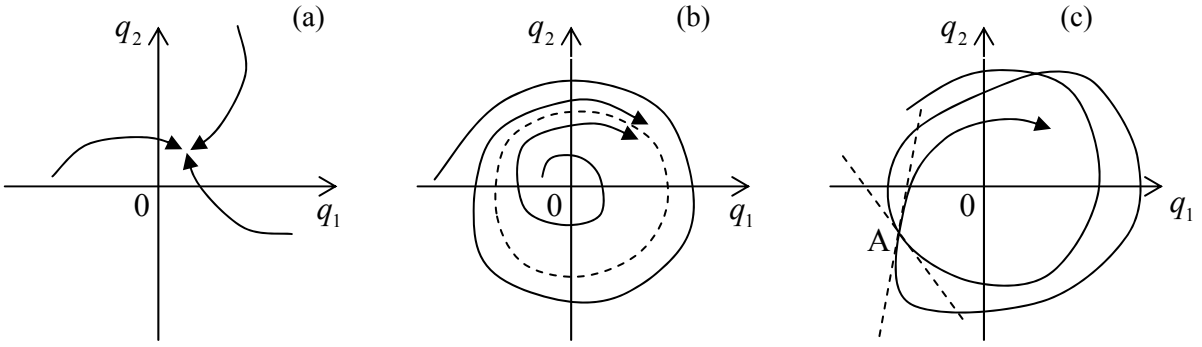

Fig. 9.6. Attractors in dynamical systems: (a) a fixed point, (b) a limit cycle, and (c) a strange attractor.

However, in the case described by Eqs. (13), this is clearly impossible, because according to these equations, the tangent slope on the phase plane is a unique function of point coordinates $\{q_1, q_2\}$:

$$\frac{dq_1}{dq_2} = \frac{f_1(q_1, q_2)}{f_2(q_1, q_2)}. \tag{9.14}$$

Thus, in this case the deterministic chaos is impossible.[13] It becomes, however, readily possible if the right-hand parts of a system similar to Eq. (13) depend either on other variables of the system or time. For example, if we consider the first two differential equations of system (10b), in the case $f_0 = 0$ they have the structure of the system (13) and hence chaos is impossible, even at $\delta < 0$ when (as we know from Sec. 4.4) the system allows self-excitation of oscillations – leading to a limit-cycle attractor. However, if $f_0 \neq 0$, this argument does not work any longer and (as we have already seen) the system may have a strange attractor – which is, for dynamic systems, a synonym for the deterministic chaos. Thus, chaos is possible in dynamic systems that may be described by three or more differential equations of the first order.[14]

9.3. Chaos in Hamiltonian systems

The last analysis is of course valid for Hamiltonian systems, which are just a particular type of dynamic systems. However, one may wonder whether these systems, that feature at least one first integral of motion, H = const, and hence are more "ordered" than the systems discussed above, can exhibit chaos at all. The question is yes, because such systems still can have mechanisms for an exponential growth of a small initial perturbation.

[13] A mathematically-strict formulation of this statement is called the Poincaré-Bendixon theorem, which was proved by I. Bendixon as early as in 1901.

[14] Since a typical dynamic system with one degree of freedom is described by two such equations, the number of the first-order equations describing a dynamic system is sometimes called the number of *half-degrees of freedom*. This notion is very useful and popular in statistical mechanics – see, e.g., SM Sec. 2.2 and on.

As the simplest way to show it, let us consider a so-called *mathematical billiard*, i.e. a ballistic particle (a "ball") moving freely by inertia on a horizontal plane surface ("table") limited by rigid impenetrable walls. In this idealized model of the usual game of billiards, ball's velocity $\mathbf{v}$ is conserved when it moves on the table, and when it runs into a wall, the ball is elastically reflected from it as from a mirror,[15] with the reversal of the sign of the normal velocity v_n, and conservation of the tangential velocity v_τ, and hence without any loss of its kinetic (and hence the full) energy

$$E = H = T = \frac{m}{2}v^2 = \frac{m}{2}\left(v_n^2 + v_\tau^2\right). \tag{9.15}$$

This model, while being a legitimate 2D dynamic system,[16] allows geometric analyses for several simple table shapes. The simplest case is a rectangular billiard of area $a \times b$ (Fig. 7), whose analysis may be readily carried out by the replacement of each *ball* reflection event with the mirror reflection of the *table* in that wall – see dashes lines in panel (a).

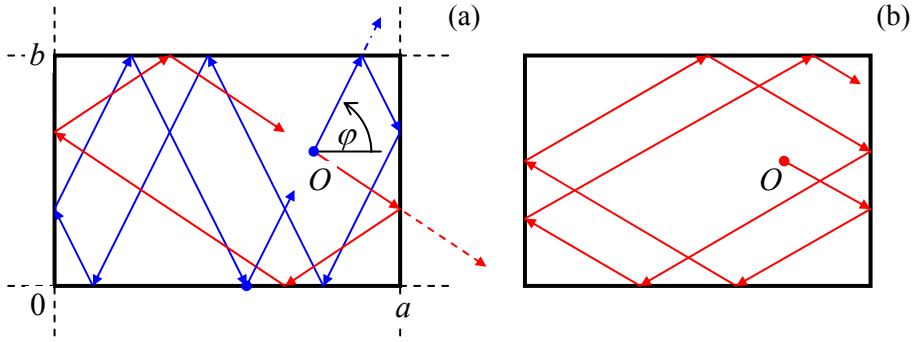

Fig. 9.7. Ball motion on a rectangular billiard at (a) a commensurate, and (b) an incommensurate launch angle.

Such analysis (left for reader' pleasure :-) shows that if the tangent of the ball launching angle φ is commensurate with the side length ratio,

$$\tan\varphi = \pm\frac{m}{n}\frac{b}{a}, \tag{9.16}$$

where n and m are non-negative integers without common integer multipliers, the ball returns exactly to the launch point O, after bouncing m times from each wall of length a, and n times from each wall of length b. (Red lines in Fig. 7a show an example of such trajectory for $n = m = 1$, while blue lines, for $m = 3$, $n = 1$.) Thus the larger is the sum $(m + n)$, the more complex is such closed trajectory - "orbit".

Finally, if $(n + m) \to \infty$, i.e. $\tan\varphi$ and b/a are incommensurate (meaning that their ratio is an irrational number), the trajectory covers all the table area, and the ball never returns exactly into the launch point. Still, this is not the real chaos. Indeed, a small shift of the launch point shifts all the trajectory fragments by the same displacement. Moreover, at any time t, each of Cartesian components $v_j(t)$ of the ball's velocity (with coordinate axes parallel to the table sides) may take only two values, $\pm v_j(0)$, and hence may vary only as much as the initial velocity is being changed.

[15] A more scientific-sounding name for such a reflection is *specular* (from Latin "speculum" meaning a metallic mirror).

[16] Indeed, it is fully described by Lagrangian function $L = mv^2/2 - U(\boldsymbol{\rho})$, with $U(\boldsymbol{\rho}) = 0$ for 2D radius-vectors $\boldsymbol{\rho}$ belonging to the table area, and $U(\boldsymbol{\rho}) = +\infty$ outside of the area.

In 1963, Ya. Sinai showed that the situation changes completely if an additional wall, in the shape of a circle, is inserted into the rectangular billiard (Fig. 8). For most initial conditions, ball's trajectory eventually runs into the circle (see the red line on panel (a) as an example), and the further trajectory becomes essentially chaotic. Indeed, let us consider ball's reflection from the circle-shaped wall – Fig. 8b. Due to the conservation of the tangential velocity, and the sign change of the normal velocity component, the reflection obeys the mechanical analog of the Snell law (cf. Fig. 7.12 and its discussion): $\theta_r = \theta_i$. Figure 8b shows that as the result, a small difference $\delta\varphi$ between the angles of two close trajectories (as measured in the lab system), doubles by magnitude at each reflection from the curved wall. This means that the small deviation grows along the ball trajectory as

$$\left|\delta\varphi(N)\right| \sim \left|\delta\varphi(0)\right| \times 2^N = \left|\delta\varphi(0)\right| e^{N \ln 2}, \tag{9.17}$$

where N is the number of reflections from the convex wall.[17] As we already know, such exponential divergence of trajectories, with a positive Lyapunov exponent, is the sign of deterministic chaos.[18]

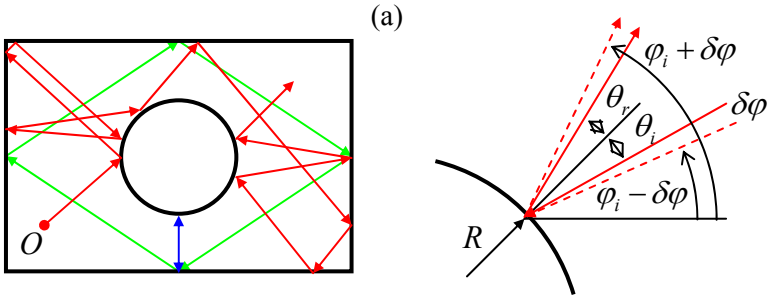

Fig. 9.8. (a) Motion on a Sinai billiard table, and (b) the mechanism of the exponential divergence of close trajectories.

The most important new feature of the dynamic chaos in Hamiltonian systems is its dependence on initial conditions. (In the systems discussed in the previous two previous sections, that lack the integrals of motion, the initial conditions are rapidly "forgotten", and the chaos is usually characterized after cutting out the initial transient period – see, e.g., Fig. 4.) Indeed, even a Sinai billiard allows periodic motion, along closed orbits, at certain initial conditions – see the blue and green lines in Fig. 8a as examples. Thus the chaos "depth" in such systems may be characterized by the "fraction"[19] of the phase space of initial parameters (for a 2D billiard, the 3D space of initial values of x, y, and φ) resulting in chaotic trajectories.

This conclusion is also valid for Hamiltonian systems that are met in experiments more frequently than the billiards, for example, coupled nonlinear oscillators without damping. Perhaps, the

[17] Superficially, Eq. (17) is also valid for a plane wall, but as was discussed above, a billiard with such walls features a full correlation between sequential reflections, so that angle φ always returns to its initial value. In a Sinai billiard, such correlation disappears. Because of that, concave walls may also make a billiard chaotic. A famous example is the *stadium billiard*, suggested by L. Bunimovich, with two straight, parallel walls connecting two semi-circular, concave walls. Another example, which allows a straightforward analysis, is the *Hadamard billiard*: an infinite (or rectangular) table with non-horizontal surface of negative curvature.

[18] Billiards are also a convenient platform for a discussion of a conceptually important issue of quantum properties of classically chaotic systems (sometimes improperly named "quantum chaos").

[19] Actually, quantitative characterization of the fraction is not trivial, because it may have fractal dimensionality. Unfortunately, due to lack of time I have to refer the reader interested in this issue to special literature, e.g., the monograph by B. Mandelbrot (cited above) and references therein.

earliest and the most popular example is the so-called *Hénon-Heiles* system,[20] which may be descrbed by the following Lagrangian function:

$$L = \frac{m_1}{2}\left(\dot{q}_1^2 - \omega_1^2 q_1^2\right) + \frac{m_2}{2}\left(\dot{q}_2^2 - \omega_2^2 q_2^2\right) - \varepsilon\left(q_1^2 - \frac{1}{3}q_2^2\right)q_2 . \tag{9.18}$$

Hénon-Heiles system

It is straightworward to use Eq. (18) to derive the Lagrangian equations of motion,

$$\begin{aligned} m_1\left(\ddot{q}_1 + \omega_1^2 q_1\right) &= -2\varepsilon q_1 q_2 , \\ m_2\left(\ddot{q}_2 + \omega_2^2 q_2\right) &= -\varepsilon\left(q_1^2 - q_2^2\right), \end{aligned} \tag{9.19}$$

and find its first integral of motion (physically, the energy conservation law):

$$H = E = \frac{m_1}{2}\left(\dot{q}_1^2 + \omega_1^2 q_1^2\right) + \frac{m_2}{2}\left(\dot{q}_2^2 + \omega_2^2 q_2^2\right) + \varepsilon\left(q_1^2 - \frac{1}{3}q_2^2\right)q_2 = \text{const} . \tag{9.20}$$

In the conext of our discussions in Chapter 4 and 5, Eqs. (19) may be readily interpreted as those describing two oscillators, with small-oscillation eigenfrequencies ω_1 and ω_2, nonlinearly coupled only as described by the terms in the right-hand parts of the equations. This means that as the oscillation amplitudes $A_{1,2}$, and hence the total energy E of the system, tend to zero, the oscillator subsystems are virtually independent, each performing sinusoidal oscillations at its own frequency. This observation suggestes a convenient way to depict the system motion.[21] Let us consider a Poincaré plane for one of the oscillators (say, with coordinate q_2), similar to that discussed in Sec. 2 above, with the only difference is that (because of the absence of an explicit function of time in system's equations), the trajectory on the $[q_2, \dot{q}_2]$ plane is highlighted at the moments when $q_1 = 0$.

Let us start from the limit $A_{1,2} \to 0$, when oscillations of q_2 are virtually sinusoidal. As we already know (see Fig. 4.9 and its discussion), if the representation point highlighting was perfectly synchronous with frequency ω_2 of the oscillations, there would be only one point on the Poincaré plane – see, e.g. the right top plane in Fig. 4. However, at the q_1 – initiated highlighting, there is not such synchronism, so that each period, a different point of the elliptical (at the proper scaling of the velocity, circular) trajectory is highlighted, so that the resulting points, for certain initial conditions, reside on a circle of radius A_2. If we now vary the initial conditions, i.e. redistribute the initial energy between the oscillators, but keep the total energy E constant, on the Poincaré plane we get a series of ellipses.

Now, if the initial energy is increased, nonlinear interaction of the oscillations start to deform these ellipses, causing also their crossings – see, e.g., the top left panel of Fig. 9. Still, below a certain threshold value of E, all Poincaré points belonging to a certain initial condition sit on a single closed

[20] It was first studied in 1964 by M. Hénon and C. Heiles as a simple model of star rotation about a gallactic center. Most studies of this equation have been carried out for the following particular case: $m_2 = 2m_1$, $m_1\omega_1^2 = m_2\omega_2^2$. In this case, introducing new variables $x \equiv \varepsilon q_1$, $y \equiv \varepsilon q_2$, and $\tau \equiv \omega_1 t$, it is possible to rewrite Eqs. (18)-(20) in parameter-free forms. All the results shown in Fig. 9 below are for this case.

[21] Generally, it has a trajectory in 4D space, e.g., that of coordinates $q_{1,2}$ and their time derivatives, although the first integral of motion (20) means that for each fixed energy E, the motion is limited to a 3D sub-space. Still, this is too much for convenient representation of the motion.

contour. Moreover, these contours may be calculated approximately, but with a pretty good accuracy, using a straighforward generalization of the small parameter method discussed in Sec. 4.2.[22]

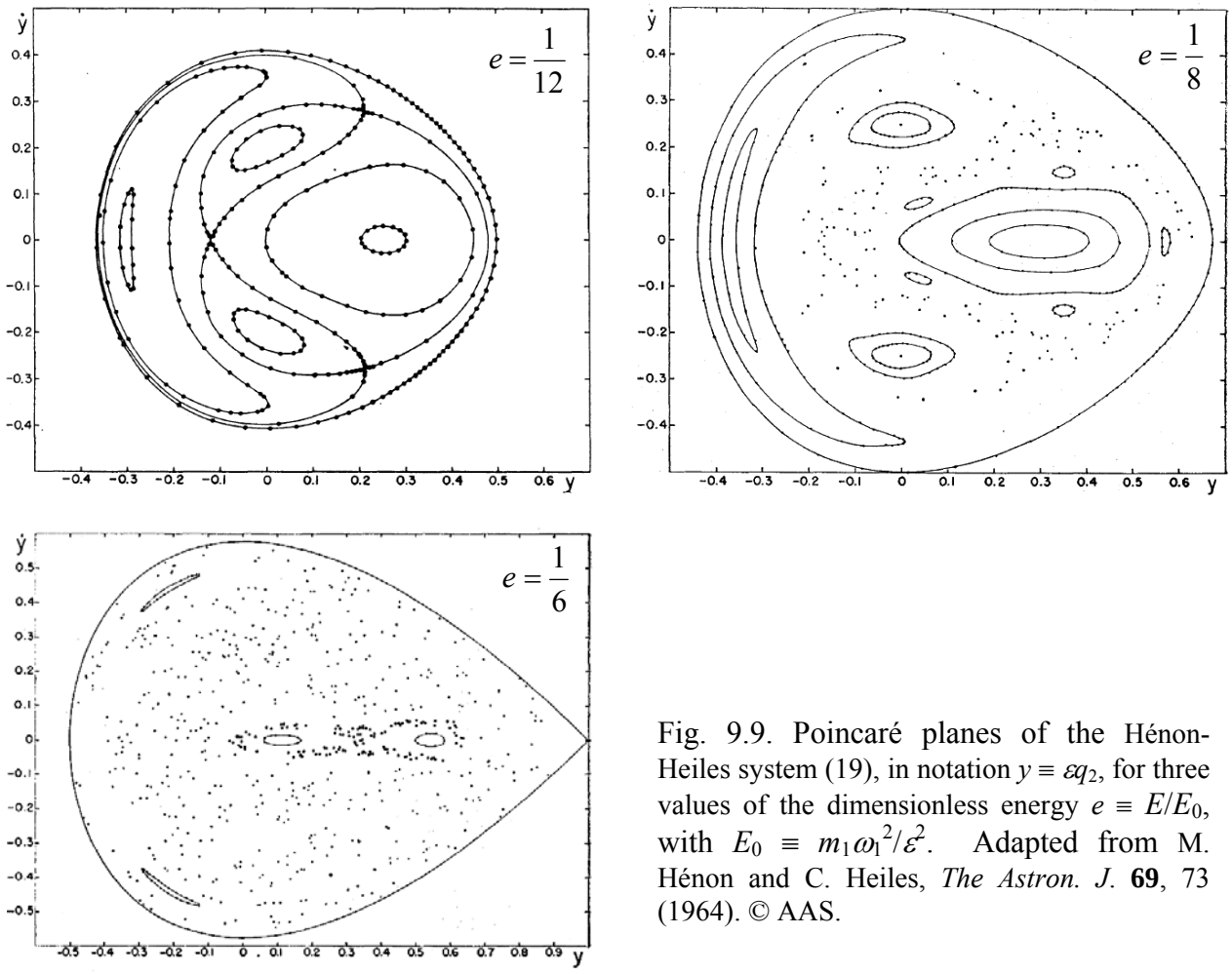

Fig. 9.9. Poincaré planes of the Hénon-Heiles system (19), in notation $y \equiv \varepsilon q_2$, for three values of the dimensionless energy $e \equiv E/E_0$, with $E_0 \equiv m_1\omega_1^2/\varepsilon^2$. Adapted from M. Hénon and C. Heiles, *The Astron. J.* **69**, 73 (1964). © AAS.

However, starting from some value of energy, certain initial conditions lead to series of points scattered over final-area parts of the Poincaré plane – see the top right panel of Fig. 9. This means that the corresponding oscillations $q_2(t)$ do not repeat from one (quasi-) period to the next one – cf. Fig. 4 for the dissipative, forced pendulum. This is chaos.[23] However, some other initial conditions still lead to closed contours. This feature is similar to Sinai billiards, and is typical for Hamiltonian systems. As the energy is increased, the larger and larger part of the Poincaré plane belongs to the chaotic motion, signifying deeper and deeper chaos.

[22] See, e.g., M. V. Berry, in: S. Jorna (ed.), *Topics in Nonlinear Dynamics*, AIP Conf. Proc. No. 46, AIP, 1978, pp. 16-120.

[23] This fact complies with the necessary condition of chaos, discussed in the end of Sec. 2, because Eqs. (19) may be rewritten as a system of four differential equations of the first order.

9.4. Chaos and turbulence

This extremely short section consists of essentially just one statement, extending the discussion in Sec. 8.5. The (re-) discovery of the deterministic chaos in systems with just a few degrees of freedom in the 1960s changed the tone of debates concerning origins of turbulence very considerably. At first, an extreme point of view that equated the notions of chaos and turbulence, became the debate's favorite.[24] However, after an initial excitement, a significant evidence of the Landau-style mechanisms, involving many degrees of freedom, has been rediscovered and could not be ignored any longer. To the best knowledge of this author, who is a very distant albeit interested observer of that field, most experimental and numerical-simulation data carry features of both mechanisms, so that the debate continues.[25] Due to the age difference, most readers of these notes have much better chances than the author to see where will this discussion end (if it does :-).[26]

9.5. Exercise problems

9.1. Generalize the reasoning of Sec. 1 to an arbitrary 1D map $q_{n+1} = f(q_n)$, with function $f(q)$ differentiable at all points of interest. In particular, derive the condition of stability of an N-point limit cycle $q^{(1)} \to q^{(2)} \to \ldots \to q^{(N)} \to q^{(1)}$.

9.2. Use the stability condition, derived in Problem 9.1, to analyze chaos excitation in the so-called *tent map*:

$$f(q) = \begin{cases} rq, & \text{for } 0 \le q \le 1/2, \\ r(1-q), & \text{for } 1/2 \le q \le 1, \end{cases} \quad \text{with } 0 \le r \le 2.$$

9.3. A dynamic system is described by the following system of ordinary differential equations:

$$\dot{q}_1 = -q_1 + a_1 q_2^3,$$
$$\dot{q}_2 = a_2 q_2 - a_3 q_2^3 + a_4 q_2 (1 - q_1^2).$$

Can it exhibit chaos at some set of constant parameters a_1-a_4?

9.4. A periodic function of time has been added to the right-hand part of the first equation of the system considered in the previous problem. Is chaos possible now?

[24] An important milestone on that way was the work by S. Newhouse *et al.*, *Comm. Math. Phys*. **64**, 35 (1978), who proved the existence of a strange attractor in a rather abstract model of fluid flow.

[25] See, e.g., U. Frisch, Turbulence: *The Legacy of A. N. Kolmogorov*, Cambridge U. Press, 1996.

[26] The reader interested in the deterministic chaos as such, may also like to have a look at a very popular book by S. Strogatz, *Nonlinear Dynamics and Chaos*, Westview, 2001.

This page is intentionally left blank